Sirolimus treatment of severe PTEN hamartoma tumor syndrome: case report and *in vitro* studies

Gordian L. Schmid[1,2], Franziska Kässner[1], Holm H. Uhlig[3], Antje Körner[1,2], Jürgen Kratzsch[4], Norman Händel[1], Fred-P. Zepp[5], Frank Kowalzik[5], Andreas Laner[6], Sven Starke[1], Franziska K. Wilhelm[1,2], Susanne Schuster[1], Adrian Viehweger[7], Wolfgang Hirsch[7], Wieland Kiess[1] and Antje Garten[1]

Background: Phosphatase and tensin homolog (PTEN) hamartoma tumor syndrome (PHTS) is caused by germ line mutations in the *PTEN* gene. Symptoms include cancer pre- disposition, immune deviations, and lipomas/lipomatosis. No causal standard therapy is available. We describe a therapeu- tic attempt with the mammalian target of rapamycin (mTOR) inhibitor sirolimus for a PHTS patient suffering from thymus hyperplasia and lipomatosis. We furthermore assessed the *in vitro* effects of sirolimus and other inhibitors on lipoma cells of the patient.

Methods: The patient underwent clinical and blood examinations and whole-body magnetic resonance imaging to assess tumor sizes. Lipoma cells of the patient were incubated with inhibitors of the phosphoinositide-3-kinase (PI3K)/AKT/ mTOR signaling pathway to analyze the effects on proliferation, adipocyte differentiation, and survival *in vitro*.

results: Sirolimus treatment improved somatic growth and reduced thymus volume. These effects diminished over the treatment period of 19 mo. Sirolimus decreased lipoma cell proliferation and adipocyte differentiation *in vitro* but did not cause apoptosis. PI3K and AKT inhibitors induced apoptosis significantly.

conclusion: Sirolimus treatment led to an improvement of the patient's clinical status and a transient reduction of the thymus. Our *in vitro* findings point to PI3K and AKT inhibitors as potential treatment options for patients with severe forms of PHTS.

Phosphatase and tensin homolog (PTEN) dephosphorylates phosphatidylinositol-3,4,5-triphosphate in the phosphoinositide 3-kinase (PI3K)/AKT/mammalian target of rapamycin (mTOR) signaling pathway. Germ line mutations in *PTEN* cause disorders, variable in severity and progression of symptoms—summarized as PTEN hamartoma tumor syndrome (PHTS) (1). The true prevalence is unknown but is estimated to be 1 in 200,000–250,000 (2) for Cowden syndrome, a subtype of PHTS. Patients develop hamartomatous tumors, intestinal polyposis, vascular malformations, and lipomas and have an increased life-time risk for breast, thyroid, and endometrial cancers (3,4). The first reported successful treatment attempt with the mTOR complex 1 (mTORC-1) inhibitor sirolimus for a patient with PHTS described a reduction of tumor masses and improvement of the patient's general state (5). More recently, an experimental oral sirolimus treatment of vascular malformation in a patient with PHTS, subtype Bannayan–Riley–Ruvalcaba Syndrome, was reported (6). We here describe the case of a child with an extreme phenotype of PHTS, including lipomatosis and severe cachexia. An individualized sirolimus treatment resulted in an improvement of the patient's symptoms. In vitro findings supported the treatment efficacy. However, after 19 mo of treatment, tumor growth accelerated again, indicating adaptation of tumor cells to mTORC-1 inhibition.

RESULTS

Clinical Findings

The patient was born as the third child of nonconsanguineous parents without a relevant family history. After birth, the patient presented as a healthy child (length: 55 cm, >90th percentile; weight: 3,900 g, >85th percentile; and head circumference: 39 cm, >97th percentile). However, the patient's state worsened into severe cachexia, with complete loss of subcutaneous adipose tissue (**Figure 1a**,**b**). A fasting glucose level of 1.9 mmol/l (35 mg/dl; reference: 3.6–5.6 mmol/l) was detected at the age of 42 mo. Attempts of oral hypercaloric nutrition failed. Parents refused nasogastric feeding. The patient's growth rate slowed down to a complete growth arrest in his fourth year (**Figure 2d**,**e**). At the age of 6 mo, he presented with dysphagia and episodes of shortness of breath due to hyperplastic tonsils and an enlarged thymus. The thymus was histologically characterized by lymphoid hyperplasia with large fractions of fatty streaks. A colonoscopy revealed an intestinal lymphoid hyperplasia (7). Furthermore, abdominal lipomatosis, fatty infiltrations of the back muscles and the upper leg, and multiple solitary lipomas were observed. Histology
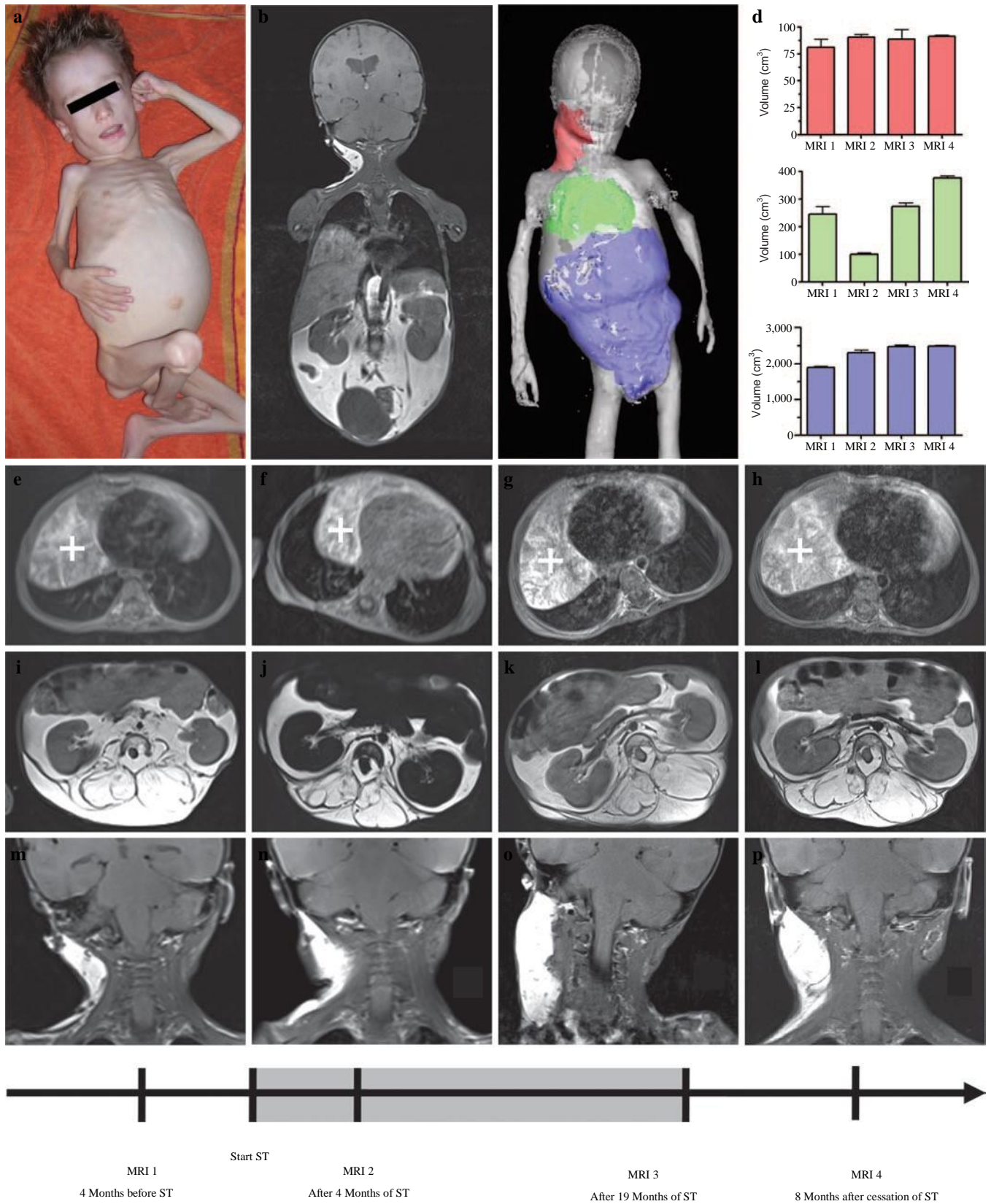
Figure 1. Clinical presentation of a boy with phosphatase and tensin homolog hamartoma tumor syndrome (PHTS). (**a**) The photograph shows the patient at the age of 3 years with cachexia and the protruded abdomen. (**b**) Retroperitoneal fat masses are apparent in the magnetic resonance imaging (MRI). (**c**) Regions of interest of the lipoma at the neck (red), the hyperplastic thymus (green), and the abdominal lipomatosis (blue) were marked in a threedimensional reconstruction of an MRI and (**d**) quantified as shown in the graphs to monitor tumor growth. (**e**–**h**) The enlarged thymus (marked with a white plus) shrank during the first 4 mo of sirolimus treatment (ST) and increased in size after 19 mo and further after cessation of therapy. (**i**–**l**) The abdominal lipomatosis did not decrease in size until the 19th mo of sirolimus therapy. (**m**–**p**) The solitary lipomas, e.g., at the right neck, did not change in volume. The shaded area on the time line indicates the duration of sirolimus treatment. Parental consent to publish this photograph was obtained by the authors.
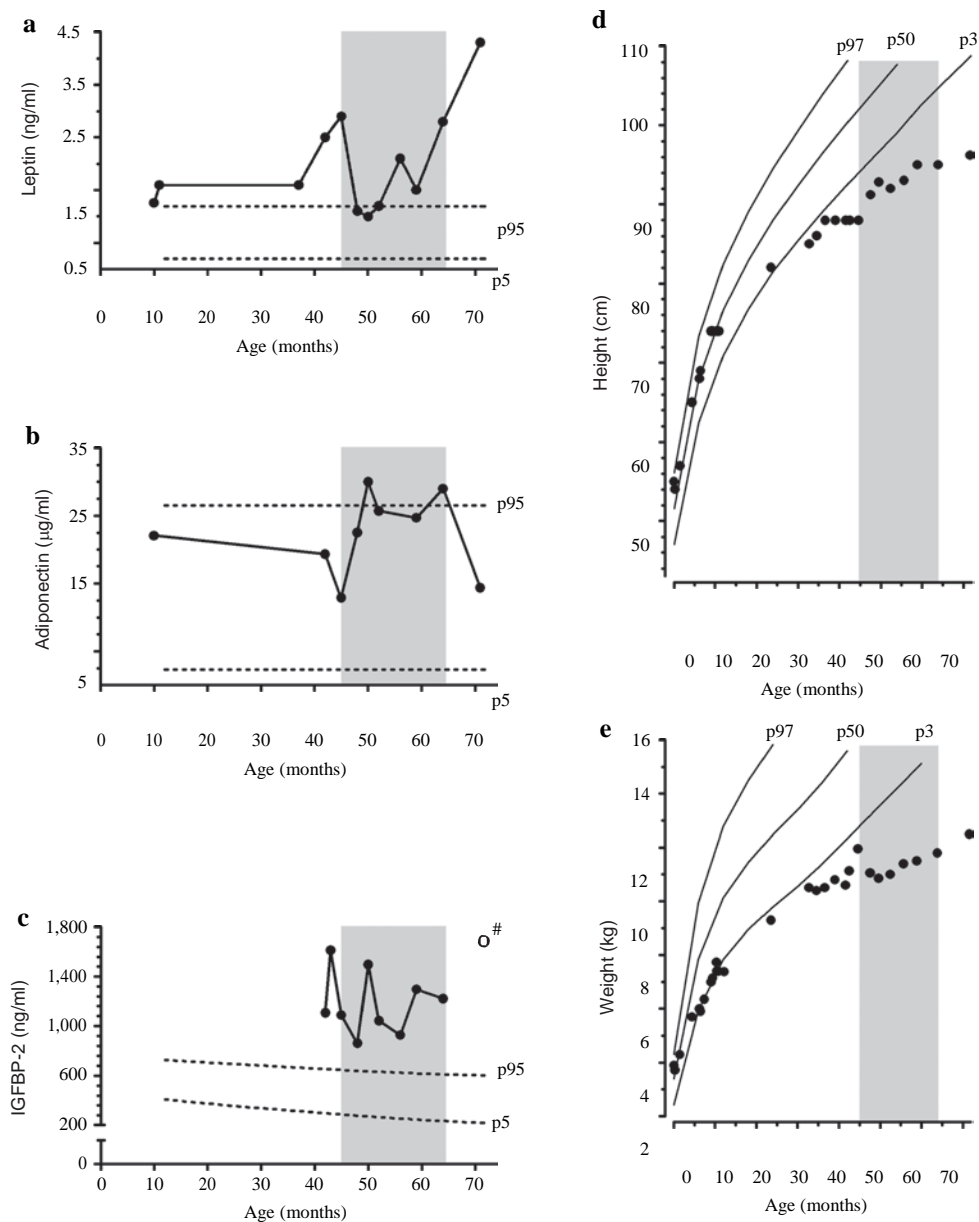

Figure 2. Serum markers and growth charts. (**a**–**c**) Serum levels of leptin, adiponectin, and insulin-like growth factor binding protein (IGFBP)-2 were measured before, during, and after sirolimus treatment. The dotted lines indicate the reference intervals. (**d**,**e**) Growth charts show the stagnated weight and the catch-up growth after initiation of sirolimus therapy. The patient's weight increased slightly during treatment. p3, 3rd percentile; p5, 5th percentile; p95, 95th percentile; p97, 97th percentile. #The open circle indicates a measurement with a concentration higher than the detectable limit, >1,680 ng/ml; the shaded areas indicate the duration of sirolimus treatment.

revealed that the benign fatty tumors were composed of about 80% white adipocytes with insular spots of multilocular cells, appearing as brown adipocytes. Subsequently, the tumors grew progressively, and additional lipomatous swellings under the skin appeared. Volumes of the tumor masses at the age of 42 mo are illustrated in the three-dimensional reconstruction of a magnetic resonance image (**Figure 1c,d** and **Supplementary Video S1** online).

Sanger sequencing of *PTEN* revealed no point mutations in the exons and flanking regions. However, a large

heterozygous *PTEN* deletion of the exons 2–9 of the nine exons was discovered in the patient's peripheral blood cells, cultured fibroblasts, and cultured lipoma cells using multiplex ligation-dependent probe amplification. The parents and siblings tested negative for the deletion. Further investigations via microarray-based comparative genomic hybridization revealed the deletion to be located between positions chr10:89,629,799 bp and chr10:89,781,899 bp. Exons 2–9 of the *PTEN* gene and about 53,400 bp downstream of the *PTEN* gene were found to be deleted.

Effects of Sirolimus Treatment
The abdominal lipomatosis led increasingly to severe compromise of mobility and breathing. Surgical lipoma reduction and chemotherapy were not justified due to the clinical state of the child. Given the published case of successful sirolimus treatment for Proteus syndrome (5), the known dose and safety profile, and the plausible mechanism of blocking being increased PI3K signaling downstream of PTEN, an individualized therapy attempt with sirolimus was initiated at the age of 46 mo. The patient received a daily oral sirolimus dose of 0.1 mg/kg body weight. Aimed serum levels (5–10 ng/ml) were reached and monitored at regular intervals.

After 4 wk of sirolimus therapy without side effects, the parents reported subjective improvement of physical and mental activity. Although serum levels of human insulin-like growth factor (IGF)-I (20.8, 14.1–34.3, and −3.33 µg/l (median, range, and mean SD score, respectively) and IGF-binding protein (IGFBP)-3 (0.32, 0.22–0.56, −8.27 µg/l) remained lower than age-matched reference values before and during sirolimus therapy, a catch-up growth of 4.8 cm (±0.57 SD score) was determined during the first 4 mo of therapy (**Figure 2d**). After 1 y of treatment, the patient was able to walk and to attend kindergarten. However, the catch-up growth slowed down. A whole-body magnetic resonance imaging conducted after 4 mo of treatment revealed a regression of the thymus (7). We measured a reduction of thymus size from 246 to 99 cm^3. The changes in the subsets of blood lymphocytes under therapy were reported earlier (7). Another whole-body magnetic resonance imaging (MRI) after 19 mo of sirolimus therapy showed recurrent growth of the thymus up to the size before therapy (273 cm^3; **Figure 1e–g**). The intestinal mucosa–associated lymphatic tissue hyperplasia improved under therapy. The growth of the abdominal lipomatosis was attenuated when comparing the 4-mo period before and after initiation of sirolimus therapy (MRI1 → MRI2, from 1,901 to 2,311 cm^3; Δ410 cm^3) with the last 15 mo of treatment (MRI2 → MRI3, from 2,311 to 2,471 cm^3; Δ160 cm^3, **Figure 1i–k**). The lipoma at the neck showed no significant changes in volume over the observed time course (**Figure 1d**,m–p). The lack of subcutaneous adipose tissue of the patient persisted, and body weight slightly increased by only 750 g. Sirolimus administration was stopped after 19 mo due to the absence of clinical benefit. Another MRI was conducted 8 mo after cessation of the sirolimus treatment. The thymus volume increased further up to 376 cm^3 (**Figure 1d,h**), but no further growth of the abdominal lipomatosis was found (**Figure 1d,l**).

Leptin and adiponectin serum levels were measured during sirolimus treatment. Interestingly, the high leptin levels decreased from 2.9 to 1.1 ng/ml (reference: 0.2–1.19 µg/l, 5th–95th percentile range) after the start of therapy but increased subsequently up to values measured initially—and greater—after treatment cessation (**Figure 2a**). Adiponectin levels increased under sirolimus treatment and persisted at median values of 25.7 (range: 22.5–30.0 µg/ml) within the upper range of the reference interval (2.33–26.50 µg/ml, 5th–95th percentile range). After cessation of sirolimus treatment, the values decreased to initial levels (**Figure 2b**). IGFBP-2 has been proposed as a diagnostic marker for the success of sirolimus therapy (5). To verify this, IGFBP-2 concentrations were measured in serum samples taken at every consultation of the patient. IGFBP-2 levels were highly variable and elevated compared with reference values (277–640 ng/ml, 5th–95th percentile range). However, no statistically significant difference between the concentrations before and under sirolimus therapy was found (**Figure 2c**).

Effects of Sirolimus *In Vitro*
We tested the effects of sirolimus, everolimus, and temsirolimus on proliferation, apoptosis, and terminal adipose differentiation of lipoma cells *in vitro*. Viability assays revealed a 42.5 ± 3.7% decrease of viability after 96 h of sirolimus treatment (100 nmol/l). Everolimus and temsirolimus showed lower effects at equimolar concentrations (**Figure 3a**). Furthermore, sirolimus caused a significant inhibition of adipose differentiation by 56.4 ± 9.1% ($P < 0.01$) at 100 nmol/l (**Figure 3b**). We found no evidence for an apoptotic/cytotoxic effect of sirolimus (**Figure 3c**) or its analogues (**Table 1**). Western blots revealed a decreased phosphorylation of the mTORC-1 target p70S6 kinase (p70S6K) after 48 h of sirolimus preincubation followed by stimulation with IGF-I. Under the same conditions, decreased levels of phospho(S636/639) insulin receptor substrate 1 (IRS1) and increased levels of phospho(S473 and T308) AKT were observed (**Figure 3e**), indicating that the feedback inhibition of AKT mediated by mTORC-1, p70S6K, and IRS1 was attenuated by sirolimus (8).

Other Inhibitors of the PI3K/AKT/mTOR Pathway
Because preferential mTORC-1 inhibitors did not induce apoptosis of lipoma cells *in vitro*, we tested other inhibitors of the PI3K/AKT/mTOR pathway. An overview is given in **Table 1**. The mTORC-1/-2 inhibitors WYE-354 (9) and KU-0063794 (10) suppressed lipoma cell viability by 76.1 ± 1.8 and 75.8 ± 0.1%, respectively, but did not induce apoptosis. The combined mTORC1/2 and PI3K inhibitor NVP-BEZ235 (11) showed similar effects. In contrast, apoptosis was induced by the PI3K inhibitor LY294002 by 74.2 ± 5.2%. Perifosine, an AKT inhibitor, decreased viability almost completely by 96.4 ± 0.6% and increased the number of apoptotic lipoma cells by 84.5 ± 0.9% (**Figure 3d**).

DISCUSSION

The clinical management of PHTS is restricted to genetic counseling, surveillance for malignancies, and surgical interventions (12,13). A causal pharmacological therapy could be based on functional compensation of the dysregulated PTEN/ AKT/mTOR signaling pathway. Two successful attempts of oral treatment with the mTORC-1 inhibitor sirolimus for patients with *PTEN* mutations have been reported (5,6). The treatment attempt described here was the first PHTS case in which lipoma adipocytes were the focus of treatment, whereas other cell types, e.g., endothelial cells, were targeted in other patients (6). Under sirolimus therapy, the growth of the patient's abdominal lipomatosis was attenuated, but the tumor volume was not reduced. These findings are in line with another case of successful sirolimus treatment for a child with a *PTEN* mutation, in which no changes in fatty tumor masses or subcutaneous adipose tissue were reported (5). We do not have clear evidence that sirolimus treatment did affect the patient's lipomatosis because the lipomatosis did not increase in size again after cessation of the sirolimus treatment. The attenuation of lipoma growth could have been simply an expression for the tragic state of cachexia in the patient, inhibiting further growth of the lipomas. In contrast, the decrease of the thymus volume under sirolimus therapy and the regrowth after cessation of treatment indicate convincingly a beneficial effect of sirolimus for the patient. The recurrence of the hyperplastic thymus after 19 mo of sirolimus therapy might be due to an acquired resistance, as has been reported before for patients treated with sirolimus analogues (14). Different mechanisms, such as hyperactivation of the AKT (14) or of the mitogen-activated protein kinase (MAPK) pathway (15) could be responsible for the potential resistance.

Marsh *et al*. (5) reported decreased IGFBP-2 serum levels under sirolimus therapy of a patient with PHTS and reelevation during cessation of therapy for 12 wk. We suspect the high IGFBP-2 levels in our patient to be an indicator of the severe state of cachexia or the decreased PTEN activity, as proposed elsewhere (16), rather than being a disease marker. Lowered leptin serum levels, as seen in our patient, might be a more relevant marker for therapy success in patients with PHTS presenting with fat-containing tumors.

When studying the effects of sirolimus *in vitro* in preadipocytes derived from a lipoma of the patient, we found a significant decrease of viability and terminal adipose differentiation under sirolimus treatment *in vitro* already at concentrations (10 nmol/l) comparable with therapeutic serum levels of the patient. In contrast with our results, other groups reported apoptotic effects of sirolimus on tumor cells with deficient p53 or p21 function (17) or at micromolar concentrations (18). Analysis of pathway activation after treatment with sirolimus revealed an attenuated activation of the mTORC-1 target p70S6K, which is in line with the observed antiproliferative effect of sirolimus on the lipoma cells. Interestingly, after 48-h treatment with sirolimus, we found decreased IRS1 serine phosphorylation and a concomitantly increased AKT phosphorylation. This AKT hyperactivation (14) could be a possible mechanistic explanation for the sirolimus resistance observed in our patient. We have to acknowledge that a limitation of our *in vitro* studies is the lack of age- and sex-matched healthy control preadipocytes to estimate the effect of the inhibitors on normal adipose tissues.

We screened additional inhibitors of the PI3K/AKT/mTOR pathway (**Table 1**) to identify putative pharmacological targets for the efficient induction of apoptosis in lipoma cells. Although long-term incubation with sirolimus was shown to exert inhibitory effects on mTORC-2 also (19), treatment with mTORC-1/-2 inhibitors led to a stronger decrease in the viability of lipoma cells. The observed proapoptotic effects of perifosine (AKT inhibitor) and LY294002 (PI3K inhibitor) on lipoma cells could be mediated by a negative regulation of the Forkhead transcription factor Foxo1 on phosphorylation by AKT (20). Inhibition of PI3K/AKT might represent a future treatment option for lipomatosis linked with defects in the *PTEN* gene. Limited potentially beneficial effects of perifosine treatment for colorectal cancer and multiple myeloma were reported (21). Nevertheless, grades 3–4 adverse effects (e.g., anemia, hand–foot syndrome, or pulmonary embolism) (21,22) limit the clinical applicability of perifosine.
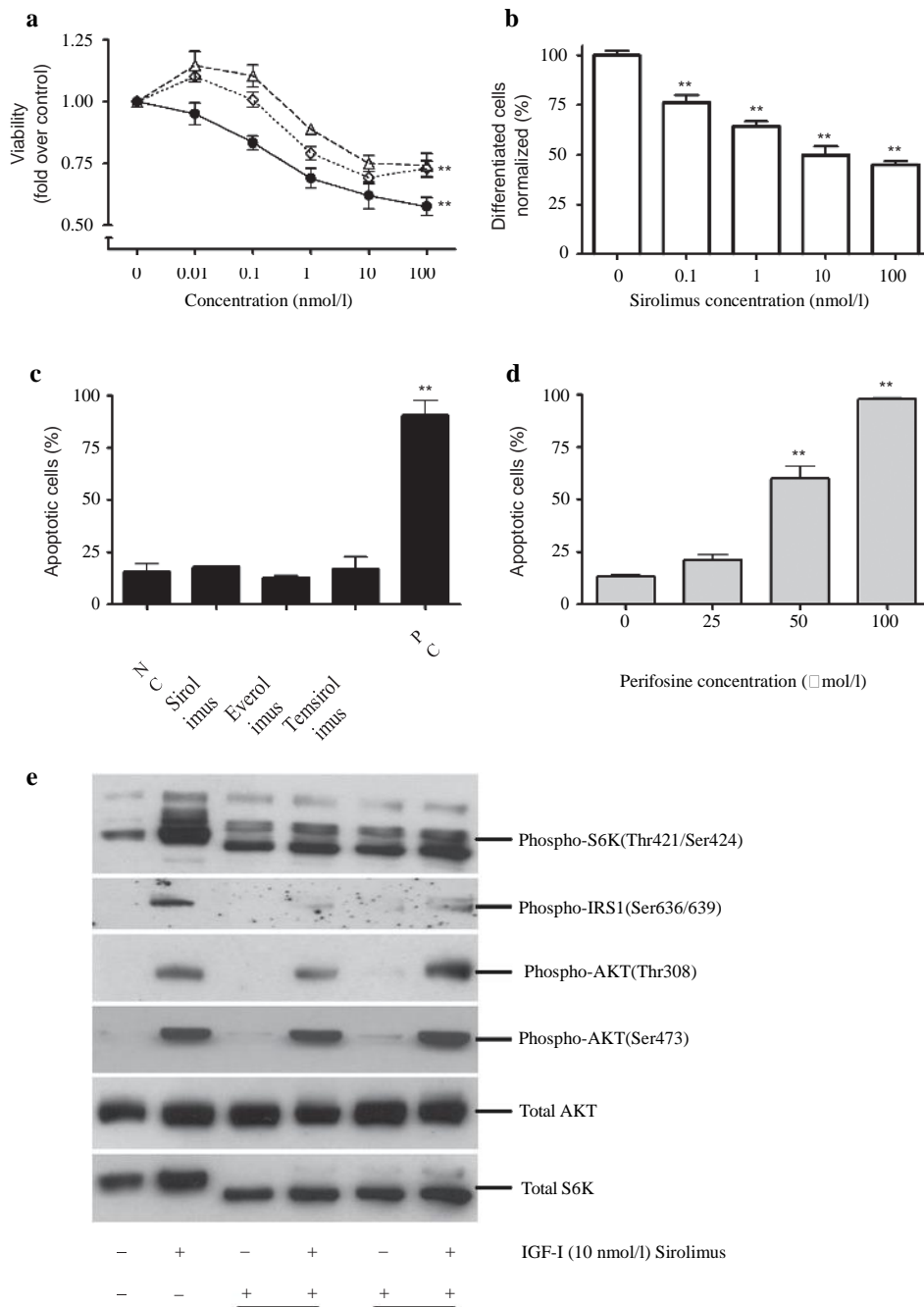
Figure 3. Inhibitor effects on proliferation, adipocyte differentiation, and apoptosis *in vitro*. (**a**) Cell viability was decreased by $42.5 \pm 3.7\%$ (mean ± SEM) by sirolimus (100 nmol/l). Analogues showed lower effects at equimolar concentrations. Data of three independent experiments normalized to 0 nmol/l values are presented. Solvent (0.1% dimethylsulfoxide)-treated cells did not differ from cells in culture medium. (Triangle, temsirolimus; diamond, everolimus; circle, sirolimus). (**b**) Sirolimus (100 nmol/l) repressed differentiation of lipoma cells into mature adipocytes by $56.4 \pm 9.1\%$ (mean ± SEM; $P < 0.01$). One representative out of three independent experiments is shown. (**c**) Sirolimus and analogues did not induce apoptosis at inhibitor concentrations of 100 nmol/l. Geneticin (G418) served as positive control and solvent (dimethylsulfoxide 0.1%) as negative control. Two independent experiments are shown. (**d**) The annexinV–fluorescein isothiocyanate/propidium iodide flow cytometry analysis revealed an increase in apoptotic lipoma cells by $84.5 \pm 0.9\%$ after 72 h of perifosine treatment. Three independent experiments performed in duplicates are shown. (**e**) The phosphorylation of p70S6K after stimulation with insulin-like growth factor (IGF)-I was inhibited by sirolimus at concentrations of 10 and 100 nmol/l. The decreased phosphorylation of insulin receptor substrate 1 (IRS1) and the concomitant stronger AKT activation might reflect the loss of the negative feedback loop of p70S6K via insulin receptor substrate 1 under sirolimus treatment. One representative out of three independent experiments is shown. $**P < 0.001$. NC, negative control; PC, positive control.

table 1. Effects of inhibitors on proliferation and apoptosis of lipoma cells in culture

Drug (concentration of maximum inhibition)	Target	Maximum inhibition of viability (%) (mean±SEM)	Change in apoptotic cells (%) (mean±SEM)	Human trials
Sirolimus (100 nmol/l)	mTORC-1	42.50±3.67**	No	Approved
Everolimus (10 nmol/l)	mTORC-1	30.71±2.55**	No	Approved
Temsirolimus (100 nmol/l)	mTORC-1	25.82±4.88*	No	Approved
WYE-354 (5 µmol/l)	mTORC-1+2	76.10±1.83**	No	Preclinical (25)
KU-0063794 (5 µmol/l)	mTORC-1+2	75.80±0.06**	No	Preclinical (25)
Wortmannin (100 µmol/l)	PI3K	40.89±3.24**	No	—
LY294002 (500 µmol/l)	PI3K	98.09±0.70**	74.22±5.21**	—
NVP-BEZ235 (10 µmol/l)	PI3K, mTORC-1+2	82.12±4.12**	No	Phase I/II (26)
Perifosine (100 µmol/l)	AKT	96.40±0.60**	84.52±0.90**	Phase III (27)

The presented data show the effects of inhibitors of the PI3K/AKT/mTOR signaling pathways on proliferation and apoptosis of the lipoma cell strain *in vitro*. Data of three independent experiments (WST-1 assays) in triplicates are shown. Apoptotic effects were assessed for the agents with a significant antiproliferative effect in three independent experiments in duplicates.

mTORC, mammalian target of rapamycin complex; PI3K, phosphoinositide-3-kinase.

*$P < 0.01$; **$P < 0.001$.

METHODS

Consent and Ethics

Written informed consent of the parents was obtained for the culture of lipoma cells, collection, and presentation of clinical data as well as for sirolimus treatment. Ethics consent for sirolimus treatment was obtained from the internal review board of the Leipzig University Hospital.

Genotyping

DNA was extracted using the FlexiGene DNA isolation kit (Qiagen, Hilden, Germany). Exons and flanking regions of *PTEN* (GenBank: NT_030059; NM_000314.4) were amplified by polymerase chain reaction and analyzed by direct DNA sequencing with the Mutation Surveyor V3.97 (SoftgeneticsLLC, State College, PA). To detect deletions/duplications of exons of *PTEN,* multiplex ligation-dependent probe amplification screening was performed (MRC-Holland, Amsterdam, The Netherlands). Break point analysis was performed using a custom-designed array-based comparative genomic hybridization of chromosome 10 (Source Bioscience, NimbleGen platform, Nottingham, UK). Further details of the method will be given on request.

MRI Reconstruction

MRI data (sequence = T1-turbo-spin-echo, echo time (TE) = 9.5 ms, repetition time (TR) = 670 ms, device: 3 tesla; Siemens, Erlangen, Germany) were assessed using the open source software Osirix-DICOM viewer (http://www.osirix-viewer.com/Contact.html). We used two-dimensional-growing brush regions of interest for segmentation of the tumor volumes (23). Volumes were segmented twice by two observers and presented as means ± SDs. The volume rendering of the MRI analysis differed slightly from routine measurements reported earlier (7).

Primary Cell Culture

Lipomas from the lumbar skin and retroperitoneal space were resected for diagnostic purposes. Remaining tissue was used to establish an adherent preadipocyte culture. A detailed protocol is given in the **Supplementary Data** online.

Adipose Differentiation

Lipoma cells were differentiated following adapted protocols (24). Sirolimus was added at the indicated concentrations. To determine the percentage of lipid-accumulating cells, triglycerides were stained with Nile red and Hoechst-33342 (both reagents from Sigma, Munich, Germany) counterstaining visualized the nuclei. Five defined, randomly chosen areas per well were counted using fluorescence microscopy. A detailed protocol is given in the **Supplementary Data** online.

Western Blots

To investigate the effect of sirolimus on the activity of mTORC-1 *in vitro*, lipoma cells were incubated with sirolimus for 48 h and subsequently stimulated with recombinant human IGF-I (Pharmacia, Uppsala, Sweden) for 15 min. After lysis, electrophoretic separation of proteins, and blotting onto nitrocellulose membranes, immunoblotting was performed to detect the amount of phosphorylated p70S6K(Thr421/Ser424), IRS1(Ser636/639), and AKT(Thr308; Ser473; all from NEB, Ipswich, MA) using standard protocols.

Cell Proliferation

The effects of the inhibitors on cell proliferation were estimated using the WST-1 assay (Roche, Mannheim, Germany) following the manufacturer's instructions. Cells were seeded at a density of 10,000 cells/cm² and incubated for 72 or 96 h with different inhibitor concentrations. The following inhibitors were used: sirolimus, everolimus, temsirolimus, wortmannin, NVP-BEZ235 (LCLaboratories, Woburn, MA), perifosine, LY294002 (Selleckchem, Munich, Germany), WYE-354, and KU-0063794 (Chemdea, Rigdewood, NJ). Absorbance was measured at 450 nm.

Induction of Apoptosis and Cell Death

Apoptosis was determined by annexinV–fluorescein isothiocyanate/propidium iodide (BD, Franklin Lakes, NJ) staining. Cells were seeded at a density of 5,000 cells/cm² in 35-mm dishes. After 24 h, cells were treated with inhibitors for 72 h. Media were changed every day. Cells were trypsinized and incubated with annexinV–fluorescein isothiocyanate and propidium iodide for 10 min at 4 °C in the dark. AnnexinV-positive and AnnexinV/propidium iodide–double positive cells were considered apoptotic/dead.

Measurement of IGFBP-2, IGFBP-3, Leptin, and Adiponectin

Serum levels of IGFBP-2, IGFBP-3, leptin, and adiponectin were determined using the IGFBP-2 enzyme immunoassay, IGFBP-3 enzyme-linked immunosorbent assay, the sensitive leptin enzyme-linked immunosorbent assay, and the adiponectin enzyme immunoassay (Mediagnost, Reutlingen, Germany) according to manufacturer's instructions. Age or age- and BMI-dependent reference intervals were transferred from manufacturer's data.

Statistics

Statistical analysis of data was performed with GraphPad Prism 5.4 software (GraphPad Software, La Jolla, CA) by applying one-way ANOVA, followed by Bonferroni's multiple comparison test. Significant differences are designated as *$P < 0.01$; **$P < 0.001$.

SUPPLEMENTARY MATERIAL

ACKNOWLEDGMENTS

STATEMENT OF FINANCIAL SUPPORT

REFERENCES

1. Eng C. PTEN: one gene, many syndromes. Hum Mutat 2003;22:183–98.
2. Nelen MR, Kremer H, Konings IB, et al. Novel PTEN mutations in patients with Cowden disease: absence of clear genotype-phenotype correlations. Eur J Hum Genet 1999;7:267–73.
3. Tan MH, Mester JL, Ngeow J, Rybicki LA, Orloff MS, Eng C. Lifetime cancer risks in individuals with germline PTEN mutations. Clin Cancer Res 2012;18:400–7.
4. Bubien V, Bonnet F, Brouste V, et al.; French Cowden Disease Network. High cumulative risks of cancer in patients with PTEN hamartoma tumour syndrome. J Med Genet 2013;50:255–63.
5. Marsh DJ, Trahair TN, Martin JL, et al. Rapamycin treatment for a child with germline PTEN mutation. Nat Clin Pract Oncol 2008;5:357–61.
6. Iacobas I, Burrows PE, Adams DM, Sutton VR, Hollier LH, Chintagumpala MM. Oral rapamycin in the treatment of patients with hamartoma syndromes and PTEN mutation. Pediatr Blood Cancer 2011;57:321–3.
7. Heindl M, Händel N, Ngeow J, et al. Autoimmunity, intestinal lymphoid hyperplasia, and defects in mucosal B-cell homeostasis in patients with PTEN hamartoma tumor syndrome. Gastroenterology 2012;142:1093–1096.e6.
8. Tremblay F, Gagnon A, Veilleux A, Sorisky A, Marette A. Activation of the mammalian target of rapamycin pathway acutely inhibits insulin signaling to Akt and glucose transport in 3T3-L1 and human adipocytes. Endocrinology 2005;146:1328–37.
9. Yu K, Toral-Barza L, Shi C, et al. Biochemical, cellular, and in vivo activity of novel ATP-competitive and selective inhibitors of the mammalian target of rapamycin. Cancer Res 2009;69:6232–40.
10. García-Martínez JM, Moran J, Clarke RG, et al. Ku-0063794 is a specific inhibitor of the mammalian target of rapamycin (mTOR). Biochem J 2009;421:29–42.
11. Maira SM, Stauffer F, Brueggen J, et al. Identification and characterization of NVP-BEZ235, a new orally available dual phosphatidylinositol 3-kinase/mammalian target of rapamycin inhibitor with potent in vivo antitumor activity. Mol Cancer Ther 2008;7:1851–63.
12. Blumenthal GM, Dennis PA. PTEN hamartoma tumor syndromes. Eur J Hum Genet 2008;16:1289–300.
13. Lopiccolo J, Ballas MS, Dennis PA. PTEN hamartomatous tumor syndromes (PHTS): rare syndromes with great relevance to common cancers and targeted drug development. Crit Rev Oncol Hematol 2007;63:203–14.
14. O'Reilly KE, Rojo F, She QB, et al. mTOR inhibition induces upstream receptor tyrosine kinase signaling and activates Akt. Cancer Res 2006;66:1500–8.
15. Carracedo A, Ma L, Teruya-Feldstein J, et al. Inhibition of mTORC1 leads to MAPK pathway activation through a PI3K-dependent feedback loop in human cancer. J Clin Invest 2008;118:3065–74.
16. Mehrian-Shai R, Chen CD, Shi T, et al. Insulin growth factor-binding protein 2 is a candidate biomarker for PTEN status and PI3K/Akt pathway activation in glioblastoma and prostate cancer. Proc Natl Acad Sci USA 2007;104:5563–8.
17. Huang S, Liu LN, Hosoi H, Dilling MB, Shikata T, Houghton PJ. p53/p21(CIP1) cooperate in enforcing rapamycin-induced G(1) arrest and determine the cellular response to rapamycin. Cancer Res 2001;61:3373–81.
18. Yellen P, Saqcena M, Salloum D, et al. High-dose rapamycin induces apoptosis in human cancer cells by dissociating mTOR complex 1 and suppress- ing phosphorylation of 4E-BP1. Cell Cycle 2011;10:3948–56.
19. Sarbassov DD, Ali SM, Sengupta S, et al. Prolonged rapamycin treatment inhibits mTORC2 assembly and Akt/PKB. Mol Cell 2006;22:159–68.
20. Matsuzaki H, Daitoku H, Hatta M, Tanaka K, Fukamizu A. Insulin-induced phosphorylation of FKHR (Foxo1) targets to proteasomal degradation. Proc Natl Acad Sci USA 2003;100:11285–90.
21. Richardson PG, Eng C, Kolesar J, Hideshima T, Anderson KC. Perifosine, an oral, anti-cancer agent and inhibitor of the Akt pathway: mechanis- tic actions, pharmacodynamics, pharmacokinetics, and clinical activity. Expert Opin Drug Metab Toxicol 2012;8:623–33.
22. Cho DC, Hutson TE, Samlowski W, et al. Two phase 2 trials of the novel Akt inhibitor perifosine in patients with advanced renal cell carcinoma after progression on vascular endothelial growth factor-targeted therapy. Cancer 2012;118:6055–62.
23. Rosset A, Spadola L, Ratib O. OsiriX: an open-source software for navigating in multidimensional DICOM images. J Digit Imaging 2004;17:205–16.
24. Wabitsch M, Brenner RE, Melzner I, et al. Characterization of a human preadipocyte cell strain with high capacity for adipose differentiation. Int J Obes Relat Metab Disord 2001;25:8–15.
25. Vilar E, Perez-Garcia J, Tabernero J. Pushing the envelope in the mTOR pathway: the second generation of inhibitors. Mol Cancer Ther 2011;10:395–403.
26. Memorial Sloan-Kettering Cancer Center, Novartis. A Phase 1b/2 Study of BEZ235 in Patients With Advanced Renal Cell Carcinoma (RCC), 2013. (http://clinicaltrials.gov/ct2/show/NCT01453595).
27. Aeterna Zentaris, Sarah Cannon Research Institute. A Phase III Randomized Study to Assess the Efficacy and Safety of Perifosine Plus Capecitabine Versus Placebo Plus Capecitabine in Patients with Refractory Advanced Colorectal Cancer, 2013. (http://clinicaltrials.gov/ct2/show/NCT01097018).